High Ion Temperature Mode in Heliotron-*E*

K. Ida,[1,2] K. Kondo,[1] K. Nagasaki,[1] T. Hamada,[1] S. Hidekuma,[1,2] F. Sano,[1]
H. Zushi,[1] T. Mizuuchi,[1] H. Okada,[1]
S. Besshou,[1] H. Funaba,[1] K. Watanabe,[1,2] and T. Obiki[1]
[1]*Plasma Physics Laboratory, Kyoto University, Uji, Kyoto, 611, Japan*
[2]*National Institute for Fusion Science, 464-01 Nagoya, Japan*
(Received 25 September 1995)

A high ion temperature T_i mode is observed for neutral beam heated plasmas in Heliotron-*E*. This high T_i mode plasma is characterized by a peaked ion temperature profile and is associated with a peaked electron density profile produced by neutral beam fueling with low wall recycling. The observed improvement in ion heat transport can be related to the radial electric field shear rather than to the rotation velocity shear in the bulk plasma.

PACS numbers: 52.55.Hc, 52.50.Gj

The high ion temperature enhanced confinement regime has been observed for super shots in TFTR [1], hot ion modes in JET and in JT-60 [2,3], and counter-NBI modes in ASDEX [4] and in JFT-2M [5]. These enhanced confinement regimes observed in many tokamaks are correlated with density peaking. However, no observation of the high ion temperature enhanced confinement regime has been reported in heliotron/torsatron or stellarator devices. Theoretically, radial electric field shear or plasma rotation shear is expected to improve confinement by suppressing microturbulence in the plasma. Then weaker particle pinch effects and a smaller improvement of energy confinement are predicted in heliotron/torsatron or stellarator devices than those in tokamaks because of strong damping of the plasma rotation due to helical ripple (only radial electric field shear due to plasma rotation shear is considered in this model) [6]. Experimentally, both bulk poloidal rotation and radial electric field were directly measured in an *H*-mode plasma in DIII-D [7]. These measurements clearly show that the bulk plasma is somewhat unrelated to the radial electric field due to a large diamagnetic drift (v_θ is in the ion diamagnetic direction which is not expected from $E \times B$ drift because E_r is negative). However, which of these, the electric field shear or the velocity shear, suppresses the turbulence has not yet been clarified because both radial electric field and velocity shear unfortunately exist in the same region in the plasma in *H* mode but not in *L* mode. Therefore it is an important issue to investigate whether density peaking and improved confinement are realized and whether a radial electric field or plasma rotation shear can reduce heat transport in heliotron/torsatron and stellarator devices. A preliminary result of the high ion temperature mode in Heliotron-*E* has been reported [8]. In this Letter we present the observation of high ion temperatures and an enhanced confinement regime in the Heliotron-*E* device and discuss the mechanism of enhanced confinement.

The Heliotron-*E* is an axially asymmetric heliotron/torsatron with poloidal period number $l = 2$, toroidal period number $m = 19$, major radius $R = 2.2$ m, magnetic field $B = 1.9$ T, and averaged minor radius $a = 21.4$ cm [9]. Heliotron-*E* has several nearly perpendicular neutral beams with 0° (five ion sources, 1.5 MW), 11° (three ion sources, 1.1 MW), and 28° injection angles (two ion sources, 0.6 MW). The neutral beams are injected into a low density target deuterium plasma produced by 53 GHz fundamental electron cyclotron heating (ECH) [10,11]. The time evolution of ion temperature profiles is measured with multichord charge exchange spectroscopy (40 spatial channels and 16.7 ms time resolution) using a charge exchange line of fully stripped carbon [12]. Electron density profiles are measured with a far-infrared interferometer [13] for *L* mode and high T_i mode discharges to study the effects of density gradient and/or radial electric field on the improvement of ion transport. In order to study global confinement, the plasma stored energy is measured with a diamagnetic loop [14]. When the neutral beams are injected into the low electron density ($n_e = 1 \times 10^{19}$ m^{-3}) target plasma produced by ECH, the central ion temperature $T_i(0)$ increases in time up to 0.8 keV with a peaked profile, which is called the high ion temperature (HIT) mode.

The characteristics of the high T_i mode are summarized in Fig. 1. The neutral beams are injected from $t = 300$ ms with an injected power of 3.2 MW into the low density target plasma produced by ECH with a magnetic axis shift ΔR of -3 or -4 cm. When there is gas puffing during the neutral beam injection period, the central ion temperature $T_i(0)$ normally decreases to 0.4 keV as $n_e(0)$ is increased (*L* mode [11]). However, when the gas puff is turned off after the neutral beam injection with low wall recycling due to boron coating, both $n_e(0)$ and $T_i(0)$ increase in time (high T_i mode) as shown in Fig. 1(a). So far these high T_i mode discharges are obtained with an inside magnetic axis shift ($\Delta R < -4$ cm). The H_α emission in high T_i mode discharges is $1/3$ of that in *L* mode discharges for the same central electron density. Figure 1(b) shows the correlation between the central ion temperature and the density peaking parameter. Here $\langle n_e \rangle$ denotes the volume-averaged electron density. In the high T_i mode discharge, the central

 0031-9007/96/76(8)/1268(4)$06.00

ion temperature increases as the electron density peaking parameter increases, although it decreases as the peaking parameter decreases in L mode. Even in high T_i mode discharges, the electron density profiles become less peaked and the central ion temperature also starts to decrease after 392 ms. As shown in Fig. 1(c), an improvement of global energy confinement is also observed during high T_i mode discharge. The stored energy of the high T_i mode discharge is higher than that of the L mode discharge by 40% for the same line-averaged electron density. Both the central ion temperature and stored energy reach a maximum at $t = 392$ ms (92 ms after the neutral beam is injected) and the central ion temperature and stored energy start to drop afterwards.

A similar phenomenon is observed when the electron density is peaked by H_2/D_2 pellet injection [15]. The central ion temperature drops to 0.3 keV associated with the increase of the central electron density after the pellet injection ($t = 333$ ms); then both the central ion temperature and electron density increase. The central ion temperature reaches 0.65 keV, which is also higher than that in the high density L mode with a similar electron density. The increase of stored energy is also observed in the discharges with H_2/D_2 pellet injection as well as the increase in the central ion temperature. The similarity between the high T_i mode and the discharges with H_2/D_2 pellet injection implies that the density gradient plays an important role in improving ion transport.

Transport analysis for L mode and high T_i mode discharges has been done to check whether the increase of the ion temperature is due to the increase of NBI power deposition or due to the improvement of transport. As shown in Fig. 1(d), the ion temperature profile is peaked at the plasma center for the high T_i mode discharge, while it is flat for L mode discharge. The central ion temperature in high T_i mode is almost twice that in the L mode, and this increase cannot be explained by the change of the power deposition. As shown in Fig. 1(e), electron density profiles are peaked at the plasma center for high T_i mode discharges where the gas puff is turned off at the onset of neutral beam injection, while it is flat for L mode discharges with continuous gas puff. The particle source due to the recycling and gas puff, $S_{R+\mathrm{puff}}$, in high T_i mode discharge is less than that in the L mode discharges by a factor of 3, while the particle source due to the neutral beams, S_{NBI}, in high T_i mode discharge is

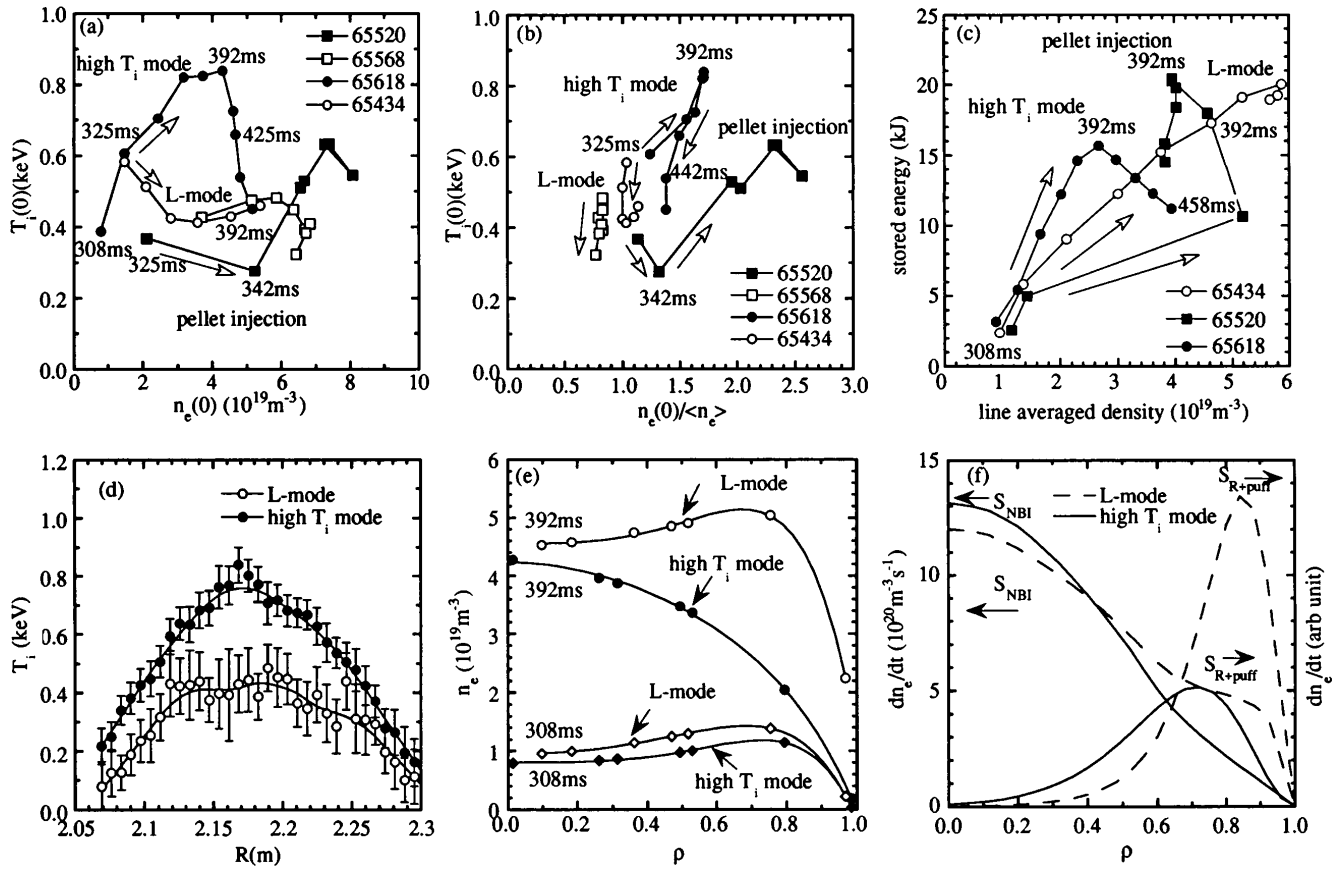

FIG. 1. (a) Central ion temperature as a function of the central electron density, (b) central ion temperature as a function of the peaking parameter of electron density profiles, (c) stored energy as a function of line averaged electron density, and radial profiles of (d) ion temperature, (e) electron density, and (f) particle source for high T_i mode, L mode, and pellet injection discharge. The data points in (a)–(c) are plotted every 16.7 ms. The magnetic axis shift is $\Delta R = -3$ cm for shots 65 520 and 65 434 and $\Delta R = -4$ cm for shots 65 618 and 65 568.

slightly more peaked than that in the L mode discharges as shown in Fig. 1(f). The total particle source in the high T_i mode discharges is more peaked than that in L mode discharges. The density peaking in high T_i mode discharges is considered to be due to the change of the particle source, at least triggered by the reduction of the edge particle source.

The power deposition of the neutral beams to electrons and ions at the plasma center in high T_i mode is only slightly higher than that in L mode, while the power deposited near the plasma edge is much less than that in L mode because of the low edge density as shown in Fig. 2(a). The increase of the central deposition power to the ions is too small to explain the significant increase of ion temperature in the high T_i mode. The total deposition power in the high T_i mode discharges is 1.8 MW (1.1 MW is absorbed by electrons and 0.7 MW is absorbed by ions) and even smaller than the 2.5 MW (1.6 MW is absorbed by electrons and 0.9 MW is absorbed by ions) in L mode discharges. The peaking of ion temperature profiles in the high T_i mode is mainly due to the reduction of the ion thermal diffusivity as shown in Fig. 2(b). The improvement of energy confinement is also seen in the global energy confinement time. The global energy confinement time, based on the diamagnetic loop measurements [14], τ_E^{diamag} is 8.7 ms in high T_i mode and 6.3 ms in L mode discharges at $n_e = 2.7 \times 10^{19}$ m^{-3}. The results of these transport analyses show an important correlation between the electron density gradient and the improvement of ion transport.

One of the effects of density peaking is to enhance the radial electric field, if the bulk rotation is kept constant. To check that, the radial electric field profiles are derived from the impurity poloidal rotation profiles with a radial force balance equation of impurities. From the radial force balance, the force due to the radial electric field E_r should be balanced by the forces due to the pressure gradient and the Lorentz force due to plasma rotation as $E_r = (1/eZ_i n_i)\partial p_i/\partial r + (B_\theta v_\phi - B_\phi v_\theta)$, where p is pressure, B_θ and B_ϕ are the poloidal and toroidal magnetic fields, and v_θ and v_ϕ are the poloidal and toroidal rotation velocities. The suffix i stands for the species; $i =$ H for bulk hydrogen and $i =$ C for carbon impurity. Z_i is the atomic charge of bulk ($Z_{\text{H}} = 1$) or carbon impurities ($Z_{\text{C}} = 6$). In a heliotron/torsatron device, toroidal rotation is damped by parallel viscosity [16], $v_\phi \sim 0$; then $E_r \sim (1/eZ_i n_i)\partial p_i/\partial r - B_\phi v_{\theta i}$.

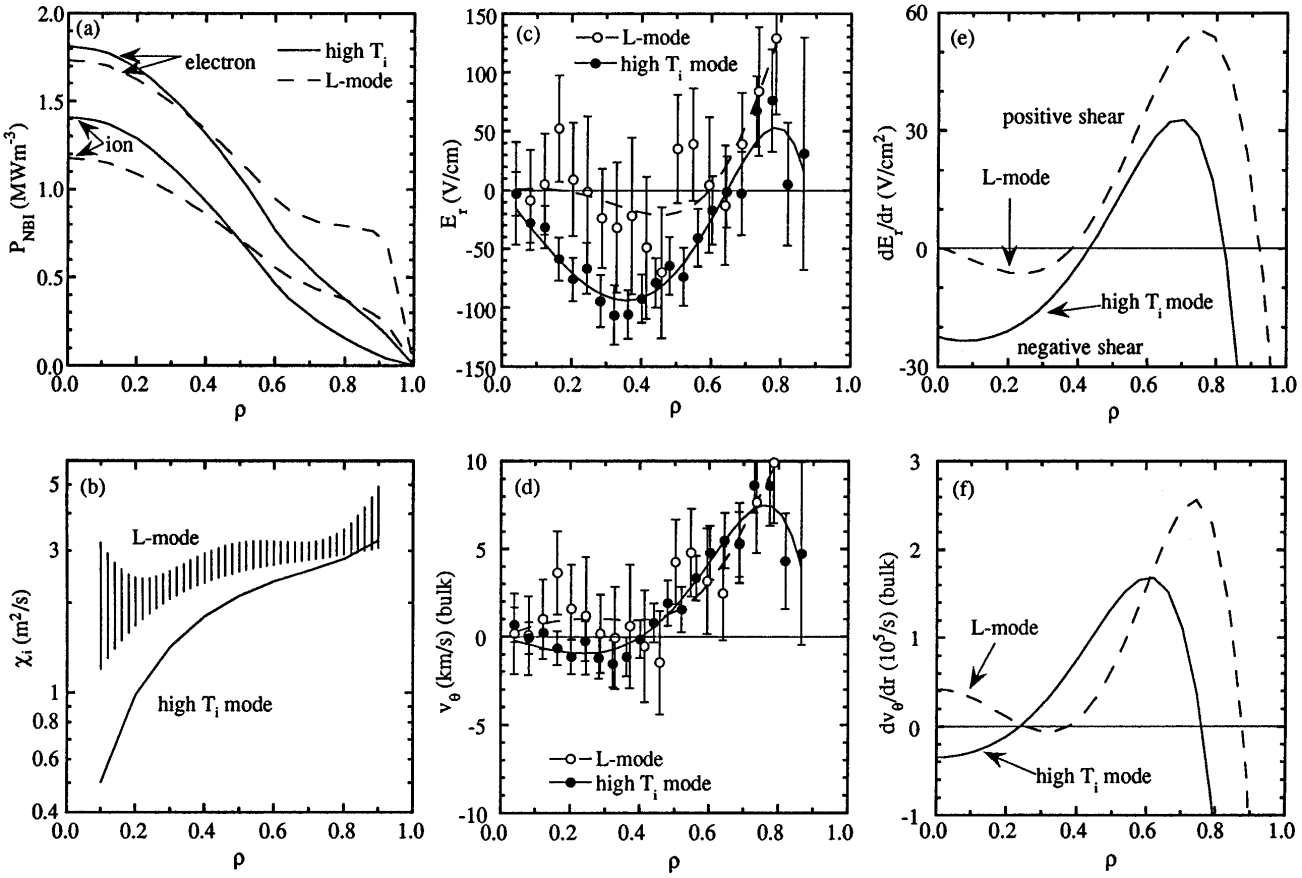

FIG. 2. Radial profiles of (a) power deposition of the neutral beam, (b) ion thermal diffusivity, (c) radial electric field, (d) bulk poloidal rotation velocity, (e) radial electric field shear, (f) rotation velocity shear for the L mode (65 434) and the high T_i mode discharge (65 618) at $t = 392$ ms. A positive value indicates rotation in ion diamagnetic direction (positive E_r). In (b), the scatter of the thermal diffusivity in various L mode discharges for similar density and heating power are plotted with error bars.

Poloidal rotation profiles of impurity ions, $v_{\theta C}(R)$, are measured and the radial electric field E_r is calculated with $E_r = (1/eZ_C n_C)\partial p_C/\partial r - B_\phi v_{\theta C}$. The bulk poloidal rotation velocity is estimated from the radial electric field and bulk pressure gradient measured as $v_{\theta H} = (1/eB_\phi Z_H n_H)\partial p_H/\partial r - E_r/B_\phi$. Here it should be noted that the diamagnetic drift velocity of the bulk ions $(1/eB_\phi Z_H n_H)\partial p_H/\partial r$ is comparable to the E_r/B_ϕ drift velocity. On the other hand, the diamagnetic drift velocity of the carbon impurity $(1/eB_\phi Z_C n_C)\partial p_C/\partial r$ is much smaller than the E_r/B_ϕ drift velocity. As shown in Figs. 2(c)–2(f), a more negative radial electric field and greater E_r shear are observed in the high T_i mode than that in L mode discharges, although the bulk poloidal rotation velocity profile in the high T_i mode is similar to that in L mode discharge. Therefore the increase of the electron density gradient is considered to result in a more negative electric field without changing the bulk poloidal rotation. A similar negative radial electric field is also observed after the pellet injection associated with density peaking. There is no impurity problem in the high T_i mode because of the boron wall coating, and the total radiation power observed in the bolometer in high T_i mode is (80–90)% of that observed in L mode.

The effect of radial electric field shear on the ion orbit is characterized by the shear parameter $u_g[= \rho_{\theta i}(\partial E_r/\partial r)/(v_{\rm th}B_\theta)]$, where $\rho_{\theta i}$ is the ion poloidal gyro radius, and $v_{\rm th}$ is ion thermal velocity [17]. Even small E_r shear has a significant effect on ion orbits, because the ion orbit banana width becomes larger due to the smaller poloidal magnetic field B_θ near the plasma center. The measured shear parameter u_g increases towards the plasma center, which is consistent with the fact that a greater reduction of ion thermal diffusivity in the high T_i mode is observed near the plasma center as shown in Fig. 2(b). The measured shear parameter u_g is -2.9 for high T_i mode, while u_g in L mode is -1.3 at $\rho = 0.2$. These results suggest a hypothesis for the mechanism of the high T_i mode in which the density gradient due to beam fueling produces a more negative radial electric field and greater E_r shear. The E_r shear reduces the turbulence [18] leading to a reduction in the ion thermal diffusivity.

It should be noted that the bulk poloidal rotation velocity profile in the high T_i mode is similar to that in L mode discharge. This fact gives the answer to the question of which is more important to suppress the turbulence and improve the confinement, electric field shear or velocity shear of bulk plasma. Figure 2(c) clearly shows that negative radial electric field shear near the plasma center ($\rho < 0.2$) only in high T_i mode, although the velocity shear of the bulk plasma at $\rho = 0.2$ shows almost no difference between the high T_i mode and the L mode. This measurement strongly suggests that the radial electric field shear is more important tan the bulk plasma velocity shear for the improvement of ion heat transport.

The magnitude of the radial electric field shear at $\rho = 0.2$ in high T_i mode is -20 V/cm^2 as shown in Fig. 2(e) and it is very similar to that observed in the counter-NBI mode in the JFT-2M tokamak [5]. These values are much smaller than edge E_r shear (-80 V/cm^2) observed in H mode. However the u_g values in the high T_i mode are comparable to or even higher than the u_g values (-1.6) observed at the periphery of plasmas in H mode [19]. Although the magnetic field structure of the Heliotron-E device is quite different from that of a tokamak, for instance, there exists a magnetic hill in most regions of Heliotron-E, the effect of the radial electric field on the improvement of confinement seems very similar between heliotron/torsatron and tokamaks. In conclusion, the high T_i mode discharge observed in Heliotron-E shows smaller thermal diffusivity than that in L mode. The mechanism of reduction of thermal diffusivity can be explained by the radial electric field shear associated with density peaking, which is produced by beam fueling for a low density target plasma with low recycling wall conditioning.

The authors acknowledge useful discussion with Dr. K. Itoh and Dr. B. J. Peterson and technical support by the Heliotron-E ECH, NBI, and machine operation groups.

[1] R. J. Fonck *et al.*, Phys. Rev. Lett. **63**, 520 (1989).
[2] H. Weisen *et al.*, Nucl. Fusion **29**, 2187 (1989).
[3] Y. Koide *et al.*, Nucl. Fusion **33**, 251 (1993).
[4] A. Kallenbach *et al.*, Nucl. Fusion **30**, 645 (1990).
[5] K. Ida *et al.*, Phys. Rev. Lett. **68**, 182 (1992).
[6] K. Itoh and S.-I. Itoh, Comments Plasma Phys. Controlled Fusion **14**, 13 (1991).
[7] J. Kim *et al.*, Phys. Rev. Lett. **72**, 2199 (1994).
[8] T. Obiki *et al.*, in *Proceedings of the 15th International Conference on Plasma Physics and Controlled Nuclear Fusion Research*, Seville, 1994, (IAEA, Vienna, 1995), Vol. 1, p. 757.
[9] K. Uo *et al.*, in *Proceedings of the 11th International Conference on Plasma Physics and Controlled Nuclear Fusion Research*, Kyoto, 1986 (IAEA, Vienna, 1987), Vol. 2, p. 355.
[10] F. Sano *et al.*, Nucl. Fusion **24**, 1103 (1984).
[11] F. Sano *et al.*, Nucl. Fusion **30**, 81 (1990).
[12] K. Ida and S. Hidekuma, Rev. Sci. Instrum. **60**, 867 (1989).
[13] H. Zushi *et al.*, Nucl. Fusion **27**, 286 (1987).
[14] S. Besshou *et al.*, Nucl. Fusion **35**, 173 (1995).
[15] T. Obiki *et al.*, in *Proceedings of the 14th International Conference on Plasma Physics and Controlled Nuclear Fusion Research*, Wurzburg, 1992 (IAEA, Vienna, 1993), Vol. 2, p. 403.
[16] K. Ida *et al.*, Phys. Rev. Lett. **67**, 58 (1991).
[17] S.-I. Itoh and K. Itoh, J. Phys. Soc. Jpn. **59**, 3815 (1990).
[18] R. J. Groebner, Phys. Fluids B **5**, 2343 (1993).
[19] K. Ida *et al.*, Phys. Rev. Lett. **65**, 1364 (1990).